Acta Crystallographica Section B
Structural Science
ISSN 0108-7681

Supramolecular structures of N^4-substituted 2,4-diamino-6-benzyloxy-5-nitrosopyrimidines

Manuel Melguizo,[a] Antonio Quesada,[a,b] John N. Low[b,c] and Christopher Glidewell[d]*

[a]Departamento de Química Inorgánica y Orgánica, Universidad de Jaén, 23071 Jaén, Spain, [b]School of Engineering, University of Dundee, Dundee DD1 4HN, Scotland, [c]Department of Chemistry, University of Aberdeen, Meston Walk, Old Aberdeen AB24 3UE, Scotland, and [d]School of Chemistry, University of St Andrews, St Andrews KY16 9ST, Scotland

Correspondence e-mail: cg@st-andrews.ac.uk

Received 10 January 2003
Accepted 29 January 2003

The molecular and supramolecular structures of eight N^4-substituted 2,4-diamino-6-benzyloxy-5-nitrosopyrimidines are discussed, along with one analogue containing no nitroso substituent. The nitroso derivatives all exhibit polarized molecular-electronic structures leading to extensive charge-assisted hydrogen bonding between the molecules. The intermolecular interactions include hard hydrogen bonds of N—H···O and N—H···N types, together with O—H···O and O—H···N types in the monohydrate of 2-amino-6-benzyloxy-4-piperidino-5-nitrosopyrimidine, soft hydrogen bonds of C—H···O, C—H···π(arene) and N—H···π(arene) types and aromatic $\pi\cdots\pi$ stacking interactions. The predominant supramolecular structure types take the form of chains and sheets, but no two of the structures determined here exhibit the same combination of hydrogen-bond types.

1. Introduction

We have recently found that in a number of 2-amino-6-benzyloxy-5-nitrosopyrimidines the supramolecular aggregation involves not only conventional hydrogen bonds of N—H···N and N—H···O types, but also those of the N—H···π(arene) type, where the arene group involved is that of the O^6-benzyl unit (Quesada, Low *et al.*, 2002; Quesada, Marchal *et al.*, 2002). Since N—H···π(arene) hydrogen bonds do not occur in all of the 2-amino-6-benzyloxy-5-nitrosopyrimidines which we have studied, we have now undertaken a systematic study of a range of such compounds, carrying a range of amine substituents at the 4-position, in an attempt to discern the conditions under which such interactions are observed. To this end, we present here a study of the molecular and supramolecular structures of (1)–(9) [see Scheme (I)]; of these, (6) has already been discussed elsewhere (Quesada, Marchal *et al.*, 2002) and we refer to it here simply for the purposes of comparison. The amine substituents at the 4-position encompass a relatively wide range of structural diversity, including primary amines bearing linear alkyl substituents [of short, (1), medium, (2) and (7), and large chain length, (3)], cyclohexyl compound (4), phenyl compound (5), and benzyl compound (6), as well as piperidino substituents in (8) and (9) as representative of secondary amines.

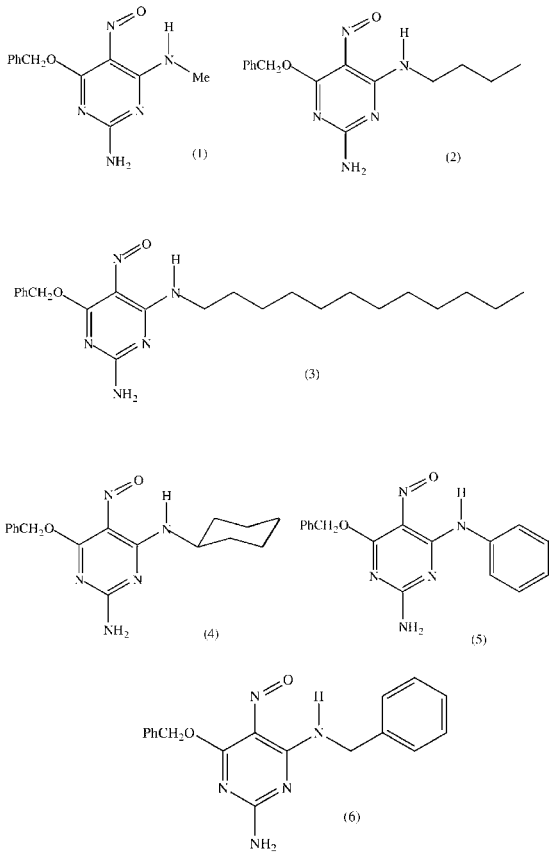

2. Experimental

2.1. Syntheses

2-Amino-4,6-dichloropyrimidine (purchased from Aldrich) was converted into 2-amino-4,6-bis(benzyloxy)pyrimidine by reaction in dimethyl sulfoxide solution with sodium benzylate, prepared *in situ* by reaction of benzyl alcohol with sodium hydride in dimethyl sulfoxide. This bis(benzyloxy) derivative was subsequently converted into (1)–(9) using methods previously described (Marchal *et al.*, 1998, 2000; Quesada *et al.*, 2000). Crystals suitable for single-crystal X-ray diffraction were grown by slow evaporation of solutions in acetone, (1) as purple plates; ethanol, (2) as blue blocks; ethanol/water (3:1 v/v), (3) as purple plates; acetonitrile/ethanol/water (1:1:1 v/v), (4) as red blocks and (9) as colourless needles; dichloromethane/methanol (1:1v/v), (5) as orange plates; acetonitrile, (7) as blue blocks; and acetone/water (1: v/v), (8)

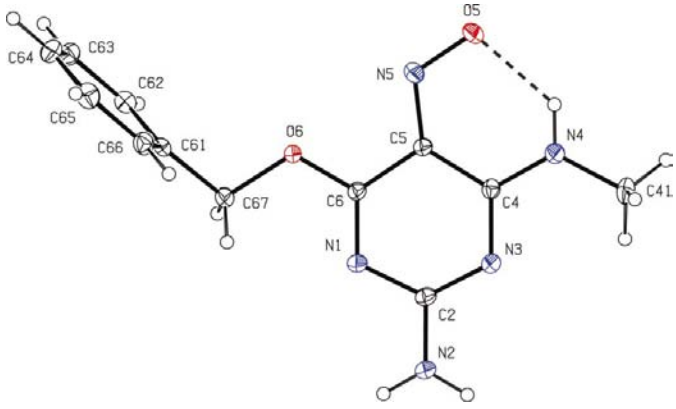

Figure 1
View of a molecule of (1) showing the atom-labelling scheme. Displacement ellipsoids are drawn at the 30% probability level.

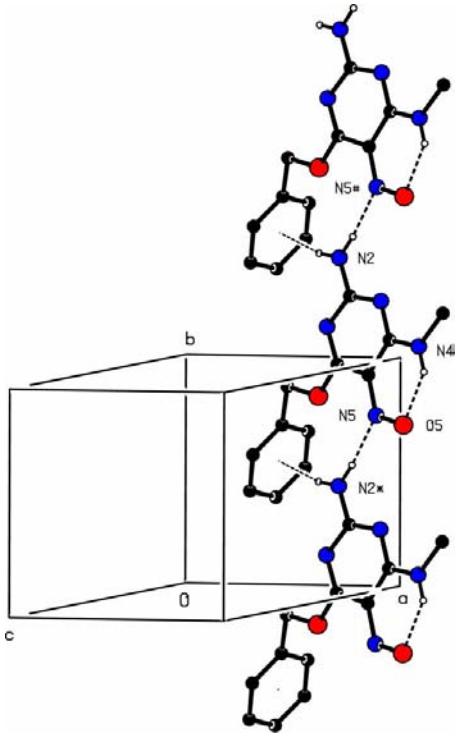

Figure 2
Part of the crystal structure of (1) showing the formation of a chain of rings along [010]. For the sake of clarity, H atoms bonded to C are omitted. The atoms marked with an asterisk (*) or a hash (#) are at the symmetry positions $(x, -1+y, z)$ and $(x, 1+y, z)$, respectively.

Table 1
Experimental details.

	(1)	(2)	(3)	(4)
Crystal data				
Chemical formula	$C_{12}H_{13}N_5O_2$	$C_{15}H_{19}N_5O_2$	$C_{23}H_{35}N_5O_2$	$C_{17}H_{21}N_5O_2$
M_r	259.27	301.35	413.56	327.39
Cell setting, space group	Orthorhombic, $P2_12_12_1$	Monoclinic, $P2_1/c$	Triclinic, $P\bar{1}$	Triclinic, $P\bar{1}$
a, b, c (Å)	7.1122 (2), 7.3873 (2), 23.3867 (7)	7.6146 (2), 13.7686 (4), 16.1215 (5)	7.3567 (4), 7.7784 (4), 21.4725 (14)	8.2656 (5), 10.6077 (6), 10.6743 (7)
α, β, γ (°)	90.00, 90.00, 90.00	90.00, 116.618 (15), 90.00	92.000 (2), 99.84 (2), 108.76 (2)	64.841 (4), 71.021 (3), 87.275 (5)
V (Å^3)	1228.74 (6)	1511.08 (8)	1141.00 (11)	796.56 (9)
Z	4	4	2	2
D_x (Mg m^{-3})	1.402	1.325	1.204	1.365
Radiation type	Mo $K\alpha$	Mo $K\alpha$	Mo $K\alpha$	Mo $K\alpha$
No. of reflections for cell parameters	1649	3424	4147	3442
θ range (°)	3.0–27.5	3.0–27.5	3.0–27.5	3.2–27.5
μ (mm^{-1})	0.10	0.09	0.08	0.09
Temperature (K)	120 (2)	120 (2)	120 (2)	120 (2)
Crystal form, colour	Plate, pink	Block, blue	Plate, purple	Block, red
Crystal size (mm)	0.30 × 0.14 × 0.07	0.35 × 0.20 × 0.15	0.18 × 0.18 × 0.08	0.12 × 0.08 × 0.06
Data collection				
Diffractometer	Kappa-CCD	Kappa-CCD	Kappa-CCD	Kappa-CCD
Data collection method	ϕ scans, and ω scans with κ offsets	ϕ scans, and ω scans with κ offsets	ϕ scans, and ω scans with κ offsets	ϕ scans, and ω scans with κ offsets
Absorption correction	Multi-scan	Multi-scan	Multi-scan	Multi-scan
T_{min}	0.954	0.966	0.976	0.974
T_{max}	0.994	0.988	0.994	0.994
No. of measured, independent and observed parameters	6981, 1649, 1323	12 361, 3424, 2616	10 984, 4147, 2819	11 753, 3442, 1528
Criterion for observed reflections	$I > 2\sigma(I)$	$I > 2\sigma(I)$	$I > 2\sigma(I)$	$I > 2\sigma(I)$
R_{int}	0.060	0.074	0.048	0.128
θ_{max} (°)	27.5	27.5	27.5	27.5
Range of h, k, l	$-9 \Rightarrow h \Rightarrow 7$ $-8 \Rightarrow k \Rightarrow 9$ $-30 \Rightarrow l \Rightarrow 30$	$-9 \Rightarrow h \Rightarrow 8$ $-17 \Rightarrow k \Rightarrow 17$ $-19 \Rightarrow l \Rightarrow 20$	$-9 \Rightarrow h \Rightarrow 9$ $-9 \Rightarrow k \Rightarrow 10$ $-27 \Rightarrow l \Rightarrow 27$	$-10 \Rightarrow h \Rightarrow 10$ $-13 \Rightarrow k \Rightarrow 13$ $-13 \Rightarrow l \Rightarrow 13$
Refinement				
Refinement on	F^2	F^2	F^2	F^2
$R[F^2 > 2\sigma(F^2)]$, $wR(F^2)$, S	0.039, 0.090, 1.09	0.045, 0.120, 1.03	0.052, 0.140, 1.01	0.063, 0.146, 0.95
No. of relections	1649	3424	4147	3442
No. of parameters	173	200	272	217
H-atom treatment	Constrained to parent site	Constrained to parent site	Constrained to parent site	Constrained to parent site
Weighting scheme	$w = 1/[\sigma^2(F_o^2) + (0.0467P)^2]$, where $P = (F_o^2 + 2F_c^2)/3$	$w = 1/[\sigma^2(F_o^2) + (0.0624P)^2 + 0.2767P]$, where $P = (F_o^2 + 2F_c^2)/3$	$w = 1/[\sigma^2(F_o^2) + (0.0752P)^2 + 0.1136P]$, where $P = (F_o^2 + 2F_c^2)/3$	$w = 1/[\sigma^2(F_o^2) + (0.0553P)^2]$, where $P = (F_o^2 + 2F_c^2)/3$
$(\Delta/\sigma)_{max}$	<0.001	<0.001	<0.001	0.001
$\Delta\rho_{max}$, $\Delta\rho_{min}$ (e Å^{-3})	0.18, −0.24	0.22, −0.29	0.22, −0.23	0.39, −0.28

	(5)	(7)	(8)	(9)
Crystal data				
Chemical formula	$C_{17}H_{15}N_5O_2$	$C_{14}H_{18}N_6O_2$	$C_{16}H_{19}N_5O_2{\cdot}H_2O$	$C_{16}H_{20}N_4O$
M_r	321.34	302.33	331.38	284.36
Cell setting, space group	Triclinic, $P1$	Monoclinic, $C2/c$	Monoclinic, $P2_1/c$	Triclinic, $P\bar{1}$
a, b, c (Å)	4.7622 (3), 5.8123 (4), 13.5635 (11)	28.3925 (6), 8.1627 (3), 15.1540 (5)	7.2557 (4), 11.4692 (7), 20.4417 (15)	6.5025 (2), 11.8006 (4), 20.7673 (10)
α, β, γ (°)	79.851 (2), 87.346 (2), 89.692 (5)	90.00, 121.97 (13), 90.00	90.00, 106.113 (3), 90.00	76.195 (14), 82.3623 (14), 77.33 (4)
V (Å^3)	369.16 (5)	2979.39 (17)	1634.27 (18)	1504.36 (10)
Z	1	8	4	4
D_x (Mg m^{-3})	1.445	1.348	1.347	1.255
Radiation type	Mo $K\alpha$	Mo $K\alpha$	Mo $K\alpha$	Mo $K\alpha$
No. of reflections for cell parameters	2993	3366	3658	6307
θ range (°)	3.0–27.4	3.2–27.5	2.9–27.4	3.2–27.4
μ (mm^{-1})	0.10	0.10	0.10	0.08
Temperature (K)	120 (2)	298 (2)	120 (2)	120 (2)
Crystal form, colour	Plate, orange	Block, blue	Plate, purple	Needle, colourless

Table 1 (continued)

	(5)	(7)	(8)	(9)
Crystal size (mm)	0.40 × 0.14 × 0.02	0.22 × 0.08 × 0.03	0.35 × 0.10 × 0.02	0.70 × 0.17 × 0.08
Data collection				
Diffractometer	Kappa-CCD	Kappa-CCD	Kappa-CCD	Kappa-CCD
Data collection method	ϕ scans, and ω scans with κ offsets	ϕ scans, and ω scans with κ offsets	ϕ scans, and ω scans with κ offsets	ϕ scans, and ω scans with κ offsets
Absorption correction	Multi-scan	None	Multi-scan	Multi-scan
T_{min}	0.895	–	0.956	0.965
T_{max}	0.998	–	0.998	0.994
No. of measured, independent and observed parameters	5085, 2993, 2348	9945, 3366, 1422	14 044, 3658, 1996	17 141, 6307, 4163
Criterion for observed reflections	$I > 2\sigma(I)$	$I > 2\sigma(I)$	$I > 2\sigma(I)$	$I > 2\sigma(I)$
R_{int}	0.071	0.065	0.094	0.054
θ_{max} (°)	27.4	27.5	27.4	27.4
Range of h, k, l	$-6 \Rightarrow h \Rightarrow 6$ $-7 \Rightarrow k \Rightarrow 7$ $-17 \Rightarrow l \Rightarrow 17$	$-28 \Rightarrow h \Rightarrow 36$ $-10 \Rightarrow k \Rightarrow 10$ $-19 \Rightarrow l \Rightarrow 16$	$-9 \Rightarrow h \Rightarrow 9$ $-14 \Rightarrow k \Rightarrow 13$ $-26 \Rightarrow l \Rightarrow 26$	$-7 \Rightarrow h \Rightarrow 8$ $-15 \Rightarrow k \Rightarrow 15$ $-26 \Rightarrow l \Rightarrow 26$
Refinement				
Refinement on	F^2	F^2	F^2	F^2
$R[F^2 > 2\sigma(F^2)]$, $wR(F^2)$, S	0.051, 0.136, 1.04	0.060, 0.145, 0.91	0.058, 0.146, 0.96	0.056, 0.161, 1.04
No. of relections	2993	3366	3658	6307
No. of parameters	217	200	217	379
H-atom treatment	Constrained to parent site	Constrained to parent site	Constrained to parent site	Constrained to parent site
Weighting scheme	$w = 1/[\sigma^2(F_o^2) + (0.0712P)^2]$, where $P = (F_o^2 + 2F_c^2)/3$	$w = 1/[\sigma^2(F_o^2) + (0.0556P)^2]$, where $P = (F_o^2 + 2F_c^2)/3$	$w = 1/[\sigma^2(F_o^2) + (0.0692P)^2]$, where $P = (F_o^2 + 2F_c^2)/3$	$w = 1/[\sigma^2(F_o^2) + (0.0891P)^2 + 0.0112P]$, where $P = (F_o^2 + 2F_c^2)/3$
$(\Delta/\sigma)_{max}$	<0.0001	<0.0001	<0.0001	<0.0001
$\Delta\rho_{max}$, $\Delta\rho_{min}$ (e Å^{-3})	0.24, −0.28	0.18, −0.20	0.24, −0.32	0.33, −0.37

Computer programs: *Kappa-CCD server software* (Nonius, 1997), *DENZO-SMN* (Otwinowski & Minor, 1997), *SHELXS*97 (Sheldrick, 1997*b*), *SHELXL*97 (Sheldrick, 1997*a*), *PLATON* (Spek, 2002), *PRPKAPPA* (Ferguson, 1999).

as purple plates. Melting temperatures: (1) 467, (2) 409, (3) 375, (4) 458, (5) 466 (dec.), (7) 429, (8) 368 and (9) 418 K.

2.2. Data collection, structure solution and refinement

Diffraction data were collected at 120 (2) K [298 (2) K for (7) only] using a Nonius Kappa-CCD diffractometer with graphite-monochromated Mo $K\alpha$ radiation (λ = 0.71073 Å). Other details of cell data, data collection and refinement are summarized in Table 1, together with details of the software employed.

For (1), the space group $P2_12_12_1$ was assigned uniquely from the systematic absences and the space group $P2_1/c$ was similarly assigned for (2) and (8): for (7) the systematic absences permitted Cc and $C2/c$ as possible space groups, of which $C2/c$ was selected, and confirmed by the subsequent analysis. Compounds (3), (4), (5) and (9) are all triclinic: space group $P\bar{1}$ was chosen for each of (3), (4) and (9), while $P1$ was selected for (5). These assignments were in each case confirmed by the successful analysis. For (9), where $Z' = 2$, ADDSYM (Spek, 2002) revealed no additional symmetry. The structures were solved by direct methods and refined with all data on F^2. A weighting scheme based upon $P = [F_o^2 + 2F_c^2]/3$ was employed in order to reduce statistical bias (Wilson, 1976). All H atoms were located from difference maps and included in the refinements as riding atoms with distances O—

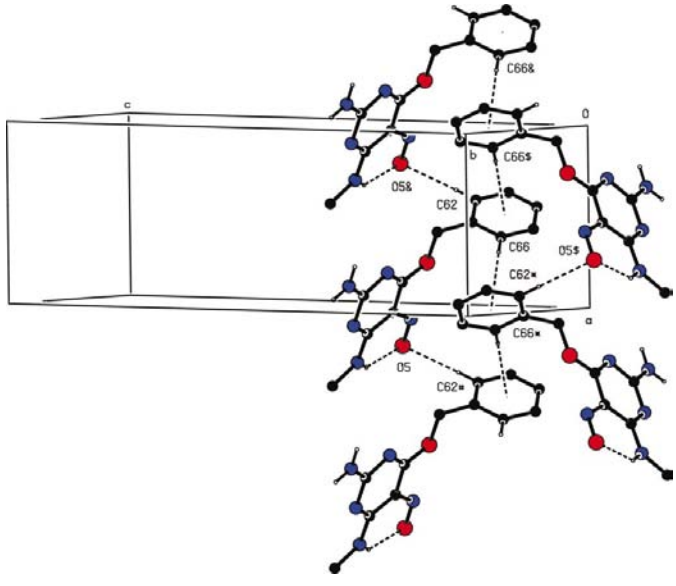

Figure 3
Part of the crystal structure of (1) showing the formation of a chain of rings along [100]. For the sake of clarity, H atoms bonded to C but not involved in the motifs shown are omitted. The atoms marked with an asterisk (*), hash (#), dollar sign ($) or ampersand (&) are at the symmetry positions $(\frac{1}{2}+x, \frac{3}{2}-y, -z)$, $(1+x, y, z)$, $(-\frac{1}{2}+x, \frac{3}{2}-y, -z)$ and $(-1+x, y, z)$, respectively.

Table 2
Selected bond lengths for (1)–(9) (Å).

$\Delta = (j - k)$.

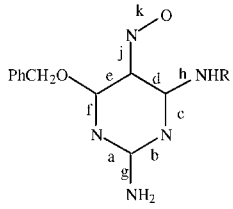

	a	*b*	*c*	*d*	*e*	*f*	*g*	*h*	*j*	*k*	Δ
(1)	1.379 (3)	1.337 (3)	1.338 (3)	1.448 (3)	1.438 (3)	1.299 (3)	1.320 (3)	1.324 (3)	1.347 (3)	1.283 (3)	0.064 (3)
(2)	1.371 (2)	1.336 (2)	1.341 (2)	1.445 (2)	1.427 (2)	1.308 (2)	1.330 (2)	1.326 (2)	1.349 (2)	1.272 (2)	0.077 (2)
(3)	1.368 (2)	1.342 (2)	1.331 (2)	1.450 (2)	1.435 (2)	1.300 (2)	1.321 (2)	1.335 (2)	1.344 (2)	1.280 (2)	0.064 (2)
(4)	1.382 (4)	1.338 (4)	1.341 (4)	1.454 (4)	1.436 (4)	1.305 (4)	1.320 (4)	1.323 (4)	1.338 (4)	1.301 (3)	0.037 (4)
(5)	1.382 (4)	1.328 (4)	1.332 (4)	1.451 (4)	1.423 (4)	1.316 (4)	1.330 (4)	1.338 (4)	1.358 (4)	1.282 (3)	0.076 (4)
(6)†	1.369 (2)	1.337 (2)	1.339 (2)	1.445 (2)	1.436 (3)	1.306 (2)	1.322 (2)	1.326 (3)	1.344 (2)	1.277 (2)	0.067 (2)
	1.366 (2)	1.344 (2)	1.338 (2)	1.454 (2)	1.426 (2)	1.298 (2)	1.319 (2)	1.324 (2)	1.347 (2)	1.275 (2)	0.072 (2)
(7)	1.378 (3)	1.333 (3)	1.339 (3)	1.443 (3)	1.422 (3)	1.303 (3)	1.326 (3)	1.326 (3)	1.352 (3)	1.279 (3)	0.073 (3)
(8)	1.371 (3)	1.343 (3)	1.345 (3)	1.461 (3)	1.443 (3)	1.305 (3)	1.324 (3)	1.331 (3)	1.348 (3)	1.282 (3)	0.066 (3)
Δ1‡	1.374 (1)	1.388 (4)	1.338 (4)	1.450 (4)	1.431 (4)	1.304 (4)	1.324 (4)	1.328 (4)	1.347 (4)	1.281 (4)	0.066 (4)
(9)	1.357 (2)	1.341 (2)	1.353 (2)	1.396 (3)	1.378 (3)	1.333 (2)	1.341 (2)	1.365 (2)	–	–	–
	1.352 (2)	1.340 (2)	1.354 (2)	1.398 (3)	1.381 (3)	1.333 (2)	1.341 (2)	1.364 (2)	–	–	–

† See Quesada, Low *et al.* (2002). ‡ Δ1 = mean values for (1)–(8).

H 1.00, N—H 0.86–88 and C—H 0.93–1.00 Å. For (1) and (5) the values of the Flack parameters (Flack, 1983), 1.7 (16) and 3.8 (16), were inconclusive (Flack & Bernardinelli, 2000): although the absolute structures could not be determined, the Friedel equivalents were not merged for (5), as this would have led to a data/parameter ratio of only 7.8.

Supramolecular analyses were made, and the diagrams were prepared, with the aid of *PLATON* (Spek, 2002). Details of molecular dimensions and bond orders are given in Tables 2 and 3, and hydrogen-bond dimensions are given in Table 4.[1] Figs. 1–19 show the molecular components with the atom-labelling schemes and aspects of the supramolecular structures.

3. Results and discussion

3.1. Molecular dimensions and conformations

In the nitrosated species (1)–(8), the bond distances involving the pyrimidine rings and its immediate substituents (Table 2) show a number of clear patterns. Firstly, the C—C bonds denoted *d* and *e* are very similar in length. Secondly, the lengths of the C—N bonds denoted *b, c, g* and *h* span only a very small range, but such that the formally single exocyclic bonds *g* and *h* are, in general, marginally shorter than the ring bonds *b* and *c*; hence, it is not possible to distinguish between those of bonds *b, c, g* and *h*, which are properly single and those which might be either double or aromatic delocalized. On the other hand, the bond denoted *f* is always significantly shorter than the rest of the C—N bonds, while bond *a* is always very much longer. Finally, bonds *j* and *k* are similar in length, although in simple neutral compounds where there is no possibility of significant electronic delocalization these distances normally differ by at least 0.20 Å (Talberg, 1977; Schlemper *et al.*, 1986) and the NO distance rarely exceeds 1.25 Å (Davis *et al.*, 1965; Bauer & Andreassen, 1972; Talberg, 1977; Schlemper *et al.*, 1986). These observations taken all together point to the polarized form (*A*) [see Scheme (II)] as the dominant contributor to the overall molecular-electronic

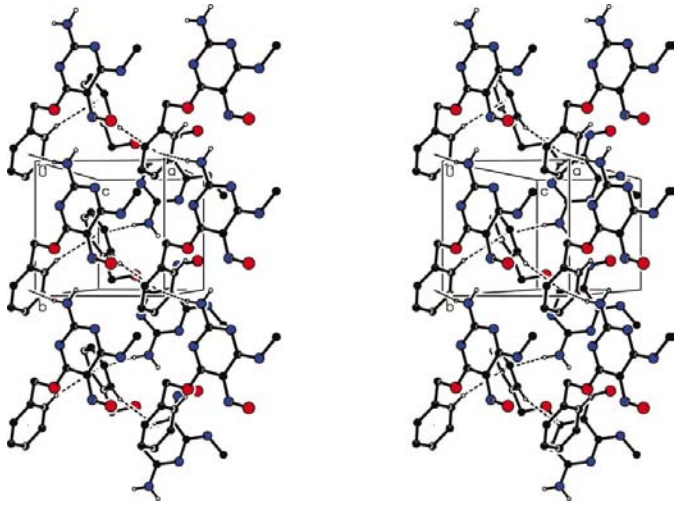

Figure 4
Stereoview of part of the crystal structure of (1) showing the N—H···π(arene) and C—H···π(arene) hydrogen bonds on opposite faces of the benzyl ring.

[1] Supplementary data for this paper are available from the IUCr electronic archives (Reference: NA0145). Services for accessing these data are described at the back of the journal.

Table 3
Selected bond orders for (1)–(9).

See structure given in Table 2.

a	*b*	*c*	*d*	*e*	*f*	*g*	*h*	*j*	*k*	Δ
(1)	1.62	1.65								
(2)	1.49	1.68	1.65	1.41	1.50	1.85	1.72	1.74	1.61	1.70
(3)	1.50	1.65	1.71	1.39	1.46	1.90	1.77	1.69	1.64	1.66
(4)	1.43	1.67	1.65	1.37	1.46	1.87	1.78	1.76	1.67	1.57
(5)	1.43	1.73	1.71	1.38	1.52	1.80	1.72	1.67	1.56	1.65
(6)†	1.50	1.68	1.67	1.41	1.46	1.86	1.77	1.74	1.64	1.68
(7)	1.45	1.70	1.67	1.42	1.53	1.88	1.74	1.74	1.59	1.67
(8)	1.49	1.64	1.63	1.34	1.42	1.87	1.75	1.71	1.61	1.65
Δ1‡	1.47	1.68	1.67	1.39	1.47	1.87	1.75	1.73	1.62	1.65
(9)†	1.56	1.65	1.59	1.66	1.76	1.70	1.65	1.52	–	–
Δ2§	−0.09	0.03	0.08	−0.27	−0.29	0.17	0.10	0.21	–	–

† Mean values, $Z' = 2$. ‡ Δ1 = mean values for (1)–(8). § Δ2 = Δ1 − value for (9).

structure, rather than the classical charge-localized form (*B*).

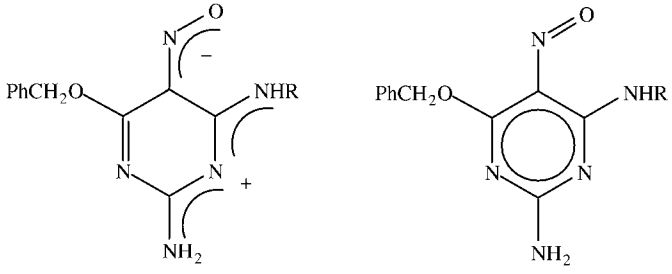

(II)

It is notable that this pattern persists even in (8), where the pyrimidine ring is distinctly non-planar: the ring-puckering parameters (Cremer & Pople, 1975; Cremer, 1984; Evans & Boeyens, 1989), Q = 0.210 (2) Å, ϕ = 29.5 (6)° and θ = 103.5 (6)° are indicative of a twist-boat conformation for the pyrimidine ring (Boeyens, 1978). Alternatively, we may define a plane through atoms C2, C4 and C6 of the pyrimidine ring in (8) and calculate the deviations from it of the other ring atoms: N1 −0.167 (3), N3 0.036 (3) and C5 0.254 (3) Å. These deviations define an approximately D_{2d} distortion of the ring, with pseudo-twofold rotation axes along the line N3···C6 and along the line joining the mid-point of the bonds N1—C2 and C4—C5. This ring distortion may be attributed to the steric repulsions between the piperidino and nitroso substituents. The piperidine ring contains an effectively planar atom N4 with a sum of bond angles at N4 of 357.5 (2)°, and a deviation of N4 from the plane C4, C41, C45 of only 0.131 (2) Å. The molecular conformation is such as to maximize the orbital overlaps implied and required by the polarized form (*A*) [Scheme (II)]. The steric clashing of the two substituents is relieved, not by any rotations of these substituents away from co-planarity with the pyrimidine ring, as might have been expected, but instead by a twisting distortion of the pyrimidine ring itself. This interpretation is supported by the structure of the non-nitrosated analogue (9), in which the two independent pyrimidine rings are planar in the absence of these distorting steric interactions, with no ring atom deviating by more than

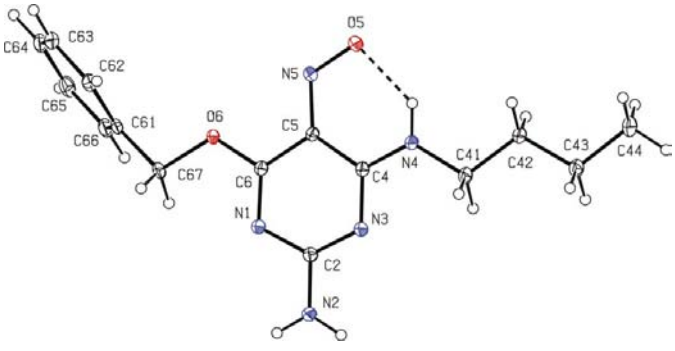

Figure 5
View of a molecule of (2) showing the atom-labelling scheme. Displacement ellipsoids are drawn at the 30% probability level.

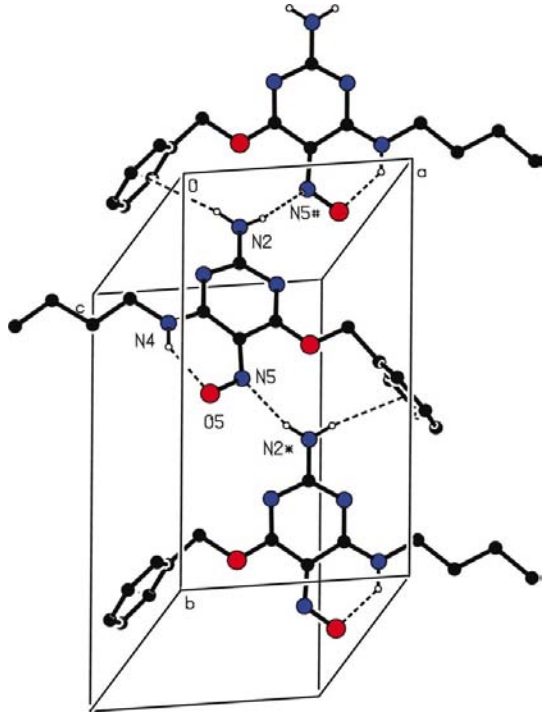

Figure 6
Part of the crystal structure of (2) showing the formation of a chain of rings along [010]. For the sake of clarity H atoms bonded to C are omitted. The atoms marked with an asterisk (*) or a hash (#) are at the symmetry positions $(1-x, \frac{1}{2}+y, \frac{1}{2}-z)$ and $(1-x, -\frac{1}{2}+y, \frac{1}{2}-z)$, respectively.

0.024 (2) Å from the planes defined by C12, C14 and C16 and by C22, C24 and C26.

The bond lengths in (9) also confirm the significance of the polarized form (*A*) in (1)–(8); in particular, the exocyclic C—N bonds *g* and *h* are much longer in (9) than in the nitrosated compounds. The important contribution of the polarized structure (*A*) in (1)–(8) thus means that any intermolecular hydrogen bonds involving either the N2 amino group or the N4 amino group as a donor and the 5-nitroso group as an acceptor can be regarded as charge-assisted hydrogen bonds (Gilli *et al.*, 1994) so that the strengths of such interactions are thereby enhanced. An alternative way to visualize the consequences of the molecular electronic structure is by means of the corresponding bond orders (Table 3), calculated using the recent re-calibration by Kotelevkii & Prezhdo (2001) of the original equation relating bond order to bond length (Gordy, 1947). The values for (1)–(8) point to the high values for bonds *f, g* and *h*, as well as the similarity of the values for bonds *j* and *k*. Perhaps more important are the comparisons of the mean values in (1)–(8) with those in the non-nitrosated compound (9), which shows clearly the effect of the nitroso group. In particular, bonds *f, g* and *h* are significantly strengthened by the introduction of the nitroso group, while bonds *d* and *e* are significantly weakened.

In each of (1)–(7) the nitroso group is essentially coplanar with the pyrimidine ring, and in each there is an intramolecular N—H···O hydrogen bond having the nitroso O as an acceptor which doubtless reinforces this tendency to coplanarity. There is thus a clear similarity in overall molecular shape between 4-amino-5-nitrosopyrimidines (*C*) on the one hand and purines (*D*) on the other [Scheme (III)].

The remaining conformational details present no unexpected features: the aliphatic chains in (2), (3) and (7) all adopt the all-*transoid* extended-chain conformation (Figs. 5, 9 and 15), while the saturated rings in (4), (8) and (9) all adopt chair conformations (Figs. 11, 18 and 20).

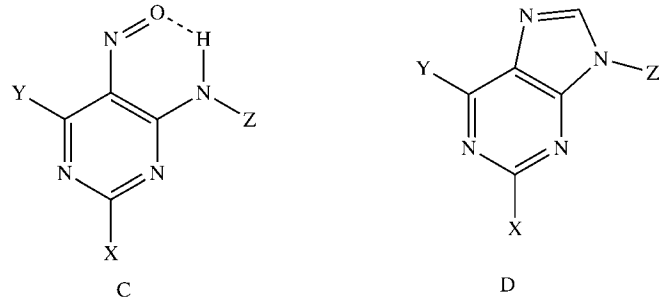

(III)

3.2. Supramolecular structures

3.2.1. 2-Amino-6-benzyloxy-4-(*N*-methylamino)-5-nitrosopyrimidine (1). Two of the amino N—H bonds in (1) (Fig. 1) are involved in intermolecular hydrogen bonds of very different types, but these act in a cooperative fashion to form a chain. The amino N2 in the molecule at (x, y, z) acts as a hydrogen-bond donor, *via* H2*A* and H2*B*, respectively, to nitroso N5, thus forming a *C*(7) chain and to the centroid Cg1 of the benzyl ring C61–C66, where both acceptors are in the molecule at $(x, 1 + y, z)$: hence a chain of rings running parallel to the [010] direction is generated by translation (Fig. 2).

Similarly, there are two quite different types of intermolecular hydrogen bond involving aromatic C—H bonds: C62 at (x, y, z) acts as a donor to nitroso O5 at $(-1 + x, y, z)$, thus generating by translation a *C*(9) chain parallel to [100]. At the same time C66 at (x, y, z) acts as a donor to the benzyl ring at $(\frac{1}{2} + x, \frac{3}{2} - y, -z)$, thus forming a spiral chain parallel to [100] generated by the 2_1 screw axis along $(x, 0.75, 0)$ (Fig. 3). The C—H···O and C—H···π(arene) hydrogen bonds thus reinforce each other in forming a chain of rings, just as the N—

Figure 7
Part of the crystal structure of (2) showing the linking of the [010] chains along by the $R_2^2(4)$ rings. For the sake of clarity H atoms bonded to C are omitted, as is the unit-cell box. The atoms marked with an asterisk (*) are at the symmetry position $(-x, 1 - y, -z)$.

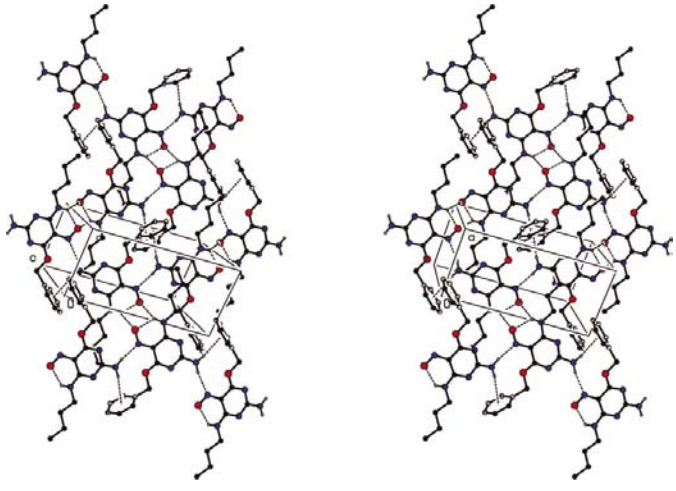

Figure 8
Stereoview of part of the crystal structure of (2) showing the linking of the [010] chains by the $R_2^2(4)$ motif. For the sake of clarity H atoms bonded to C are omitted.

H···N and N—H···π(arene) interactions do so: it may be noted here that the benzyl ring C61—C66 in the molecule at (x, y, z) accepts one X—H···π(arene) hydrogen bond (where X = C or N) on each face, from C66 at ($-\frac{1}{2}+x, \frac{3}{2}-y, -z$) and from N2 at ($x, -1+y, z$) (Fig. 4).

The combination of the [100] and [010] chains generates a (001) sheet: there are no aromatic $\pi\cdots\pi$ stacking interactions or any other direction-specific interactions between the sheets, so that the supramolecular structure as defined by the direction-specific interactions is two-dimensional.

3.2.2. 2-Amino-6-benzyloxy-4-(*N*-butylamino)-5-nitrosopyrimidine (2). As in (1), the amino N2 in (2) (Fig. 5) acts as a hydrogen-bond donor, *via* H2*A* and H2*B*, respectively, to N5 and to the centroid of the benzyl ring C61–C66 in the same molecule, which in this case is at ($1-x, -\frac{1}{2}+y, \frac{1}{2}-z$), so that the chain of rings running parallel to [010] (Fig. 6) is generated here by the 2_1 screw axis along ($\frac{1}{2}, y, \frac{1}{4}$), rather than by translation as in (1).

There are neither C—H···O nor C—H···π(arene) hydrogen bonds in the structure of (2), but instead the [010] chains are linked by one component of a three-centre N—H···(O)$_2$ hydrogen bond, in which the donor is the substituted amino N4 and the two acceptors are the nitroso O5 atoms at (x, y, z), giving the usual intramolecular $S(6)$ motif, and at ($-x, 1-y, -z$), so forming a centrosymmetric $R_2^2(4)$ ring (Fig. 7). It is interesting to note that this rather unusual motif is also observed in the sterically similar analogue of (2), having R = CH_2CH_2COOEt, rather than R = $CH_2CH_2CH_2CH_3$ (Quesada, Marchal *et al.*, 2002). The molecule at ($-x, 1-y, -z$) is a component of the [010] chain along ($-\frac{1}{2}, -y, \frac{1}{4}$), so that this $R_2^2(4)$ ring serves to link the chains along ($\frac{1}{2}, y, \frac{1}{4}$) and ($-\frac{1}{2}, -y, \frac{1}{4}$). The molecule at ($1-x, -\frac{1}{2}+y, \frac{1}{2}-z$), also a component of the ($\frac{1}{2}, y, \frac{1}{4}$) chain, similarly forms an $R_2^2(4)$ ring with the molecule at ($1+x, \frac{1}{2}-y, \frac{1}{2}+z$), which is itself a component of the [010] chain along ($\frac{3}{2}, -y, \frac{3}{4}$). In this way [010] chains are linked into a ($10\bar{2}$) sheet (Fig. 8). There are no aromatic $\pi\cdots\pi$ stacking interactions or any other direction-specific interactions between the sheets, so that the supramolecular structure as defined by the direction-specific interactions is two-dimensional.

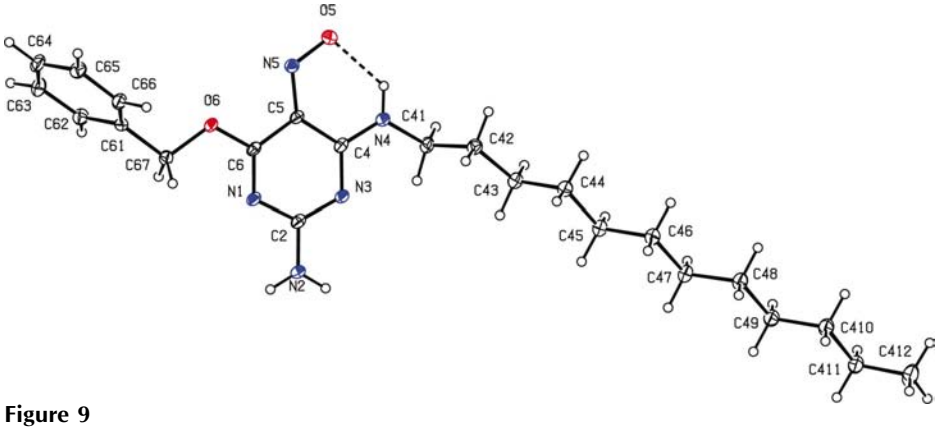

Figure 9
View of a molecule of (3) showing the atom-labelling scheme. Displacement ellipsoids are drawn at the 30% probability level.

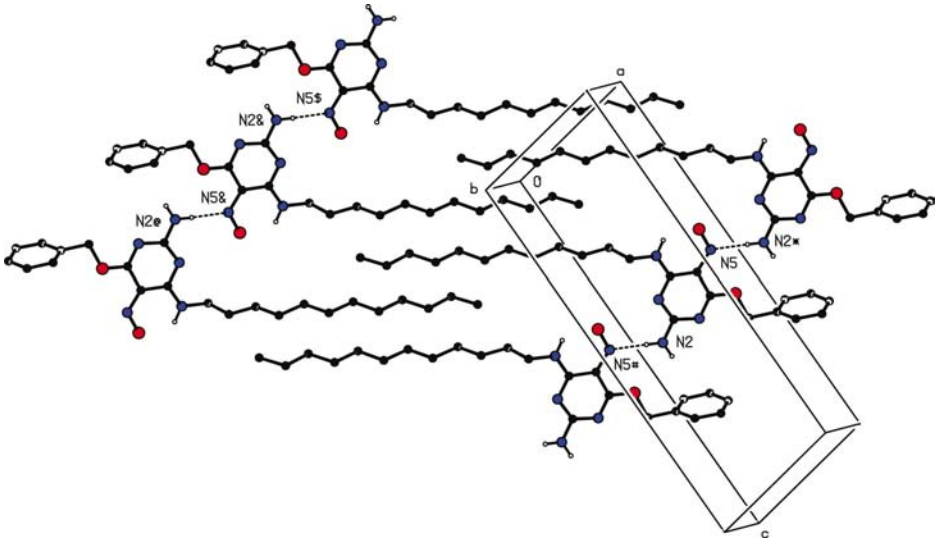

Figure 10
Part of the crystal structure of (3) showing the formation of $C(7)$ chains along [100] with interdigitated dodecyl substituents. For the sake of clarity H atoms bonded to C are omitted. The atoms marked with an asterisk (*), hash (#), dollar sign ($), ampersand (&) or at sign (@) are at the symmetry positions ($1+x, y, z$), ($-1+x, y, z$), ($-x, -y, -z$), ($-1-x, y, z$) and ($-2-x, y, z$), respectively.

3.2.3. 2-Amino-6-benzyloxy-4-(*N*-dodecylamino)-5-nitrosopyrimidine (3). In contrast to the behaviour of (1) and (2), the supramolecular structure of (3) (Fig. 9) consists of simple chains generated by translation. The amino N2 in the molecule at (x, y, z) acts as a hydrogen-bond donor, *via* H2*A*, to nitroso N5 at ($-1+x, y, z$), so forming the now-familiar $C(7)$ chain, on this occasion running parallel to [100] (Fig. 10). Pairs of [100] chains related by inversion are characterized by interdigitated dodecyl chains and the packing of these chains almost certainly dominates the overall supramolecular structure: the combination of the orientation of these chains with the all-*trans* conformation is responsible for the rather long c axis (Table 1). The other N—H bond of the amino group, H2*B*, does not participate in the hydrogen bonding, acting as a donor, neither to one of the pyrimidine ring N atoms, nor to the nitroso O, nor to the benzyl ring. There are no C—H···O or C—H···π(arene) hydrogen bonds and no aromatic $\pi\cdots\pi$ stacking interactions.

3.2.4. 2-Amino-6-benzyloxy-4-(*N*-cyclohexylamino)-5-nitrosopyrimidine (4). As with (3), the supramolecular structure of (4) (Fig. 11) consists of simple chains generated by translation. The amino N2 in the molecule at (x, y, z) acts as a hydrogen-bond donor, *via* H2*A*, to nitroso O5 at $(1 + x, y, z)$, so forming a *C*(8) chain in contrast to the *C*(7) chain in C but again running parallel to [100] (Fig. 12). The other N—H bond of this amino group, H2*B*, does not participate in the hydrogen bonding, acting as a donor, neither to one of the pyrimidine ring N atoms, nor to the nitroso N, nor to the benzyl ring. While there are no C—H···O hydrogen bonds or aromatic

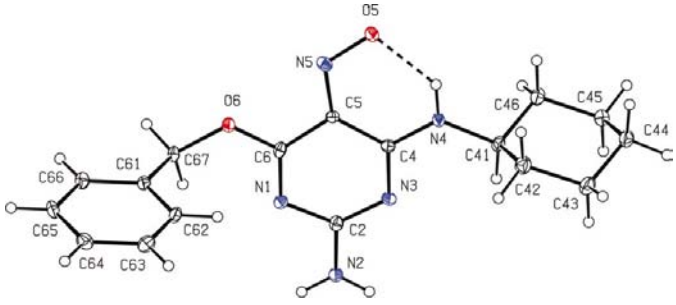

Figure 11
View of a molecule of (4) showing the atom-labelling scheme. Displacement ellipsoids are drawn at the 30% probability level.

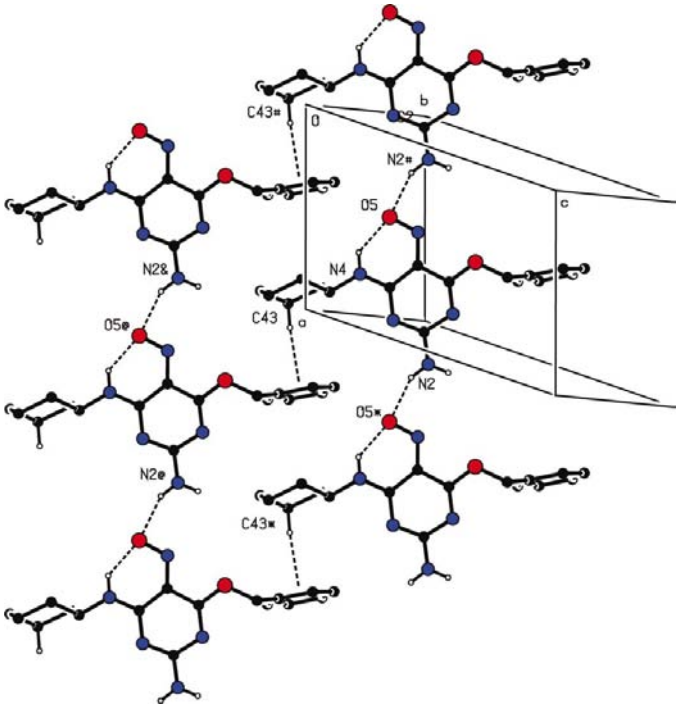

Figure 12
Part of the crystal structure of (4) showing the linking of *C*(8) chains along [100] by the C—H···π(arene) hydrogen bond. For the sake of clarity H atoms bonded to C but not involved in the motifs shown are omitted. The atoms marked with an asterisk (*), hash (#), ampersand (&) or at sign (@) are at the symmetry positions $(1 + x, y, z)$, $(-1 + x, y, z)$, $(x, y, -1 + z)$ and $(1 + x, y, -1 + z)$, respectively.

Table 4
Geometry of hydrogen bonds and short intramolecular contacts (Å, °).

D—H···*A*	H···*A*	*D*···*A*	*D*—H···*A*	Motif	Direction
(1)					
N4—H4···O5	1.95	2.618 (2)	132	*S*(6)	–
N2—H2*A*···N5^{i}	2.14	3.006 (3)	169	*C*(7)	[010]
N2—H2*B*···Cg1^{i}†	2.68	3.516 (2)	160	‡	–
C62—H62···O5^{ii}	2.45	3.379 (3)	165	*C*(9)	[100]
C66—H66···Cg1^{iii}	2.73	3.647 (2)	163	‡	–
(2)					
N4—H4···O5	2.00	2.642 (2)	129	*S*(6)	–
N4—H4···O5^{iv}	2.43	3.139 (2)	138	$R_2^2(4)$	–
N2—H2*A*···N5^{v}	2.20	3.058 (2)	164	*C*(7)	[010]
N2—H2*B*···Cg1^{v}	2.67	3.537 (2)	171	‡	–
(3)§					
N4—H4···O5	1.96	2.624 (2)	131	*S*(6)	–
N2—H2*A*···N5^{ii}	2.12	2.987 (2)	169	*C*(7)	[100]
(4)§					
N4—H4···O5	1.91	2.609 (3)	135	*S*(6)	–
N2—H2*A*···O5^{vi}	1.99	2.804 (3)	153	*C*(8)	[100]
C43—H43*B*···Cg1^{vii}	2.73	3.717 (4)	173	‡	–
(5)§					
N4—H4···O5	1.86	2.593 (3)	139	*S*(6)	–
N2—H2*A*···N5^{viii}	2.07	2.942 (3)	173	*C*(7)¶	[$\bar{1}$10]
C42—H42···N3	2.33	2.929 (4)	120	*S*(6)	–
C42—H42···O5^{viii}	2.48	3.215 (4)	133	*C*(8)¶	[$\bar{1}$10]
C67—H67*A*···N1	2.39	2.692 (4)	100	*S*(5)	–
(7)					
N4—H4···O5	2.48	3.215 (4)	133	*C*(8)¶	[$\bar{1}$10]
N2—H2*A*···N5^{ix}	2.36	3.095 (3)	144	*C*(7)††	[001]
N2—H2*B*···N63^{x}	2.14	2.980 (4)	164	*C*(10)††	[001]
C62—H62···O5^{i}	2.38	3.289 (3)	166	*C*(9)	[010]
(8)					
N2—H2*A*···N5^{ii}	2.30	3.158 (3)	165	*C*(7)	[100]
N2—H2*B*···O1	2.09	2.966 (3)	171	*D*	–
O1—H1*A*···O5^{xi}	1.87	2.791 (2)	153	$C_2^2(10)$	[010]
O1—H1*B*···N3^{xii}	1.99	2.968 (3)	167	$C_2^2(6)$	[010]
(9)					
N12—H12*A*···N21	2.29	3.105 (2)	155	*D*	–
N12—H12*B*···N23^{ii}	2.10	2.927 (2)	155	$C_2^2(6)$‡‡	[100]
N22—H22*A*···N11^{vi}	2.27	3.064 (2)	149	$C_2^2(6)$‡‡	[100]
N22—H22*B*···N13	2.10	2.920 (2)	154	*D*	–

Symmetry codes: (i) $x, 1 + y, z$; (ii) $-1 + x, y, z$; (iii) $\frac{1}{2} + x, \frac{3}{2} - y, -z$; (iv) $-x, 1 - y, -z$; (v) $1 - x, -\frac{1}{2} + y, \frac{1}{2} - z$; (vi) $1 + x, y, z$; (vii) $1 + x, y, -1 + z$; (viii) $-1 + x, 1 + y, z$; (ix) $x, 1 - y, \frac{1}{2} + z$; (x) $x, 2 - y, \frac{1}{2} + z$; (xi) $2 - x, \frac{1}{2} + y, \frac{1}{2} - z$; (xii) $1 - x, \frac{1}{2} + y, \frac{1}{2} - z$. † Cg1 is the centroid of the benzyl ring C61–C66. ‡ Graph set descriptors are not yet defined for *D*—H···π interactions. § No acceptor for N2—H2*B*. ¶ Combination of N—H···O and C—H···O hydrogen bonds generates $C_2^1(6)$ chain. †† Combination of *C*(7) and *C*(10) chains generates $R_4^4(28)$ rings. ‡‡ Combination of two $C_2^2(6)$ chains generates $R_2^2(8)$ rings.

π···π stacking interactions in the structure of (4), there is a single C—H···π(arene) hydrogen bond which links the [100] chains into a (010) sheet: atom C43 in the cyclohexyl ring at (x, y, z) acts as a hydrogen-bond donor, *via* H43*B*, to the benzyl ring in the molecule at $(1 + x, y, -1 + z)$ (Fig. 12). There are no direction-specific interactions between adjacent (010) sheets.

3.2.5. 2-Amino-6-benzyloxy-4-(*N*-phenylamino)-5-nitrosopyrimidine (5). As in (3) and (4) the supramolecular structure of (5) (Fig. 13) is generated by translation, but a hard N—H···N hydrogen bond is augmented by a soft C—H···O

hydrogen bond, involving the same pair of molecules, so producing a chain of rings in this case. The amino N2 in the molecule at (x, y, z) acts as a hydrogen-bond donor, *via* H2*A*, to nitroso N5 in the molecule at $(-1+x, 1+y, z)$, so generating by translation a $C(7)$ chain running parallel to $[\bar{1}10]$ (Fig. 14): as in (4), the other N—H bond plays no role whatsoever in the supramolecular aggregation. In addition, C42 at (x, y, z) acts as a donor to nitroso O5, also in the molecule at $(-1+x, 1+y, z)$, so generating, again by translation, a $C_2^1(6)$ chain in which O5 acts as a double acceptor. These parallel $[\bar{1}10]$ chains combine to generate an $S(6)C(7)C_2^1(6)[R_2^2(11)]$ chain of edge-fused rings. There are two short intramolecular C—H···N contacts (Table 4) which may make some contribution to the overall molecular conformation.

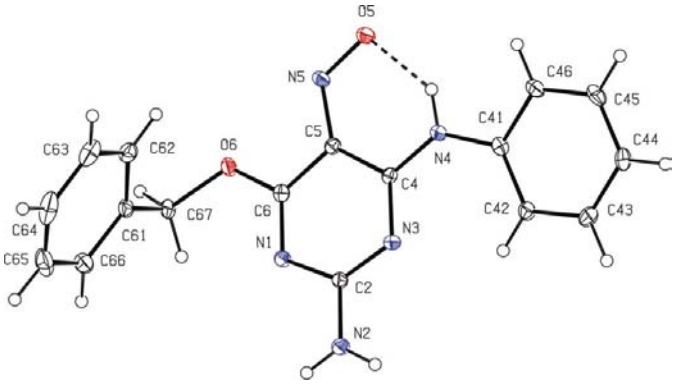

Figure 13
View of a molecule of (5) showing the atom-labelling scheme. Displacement ellipsoids are drawn at the 30% probability level.

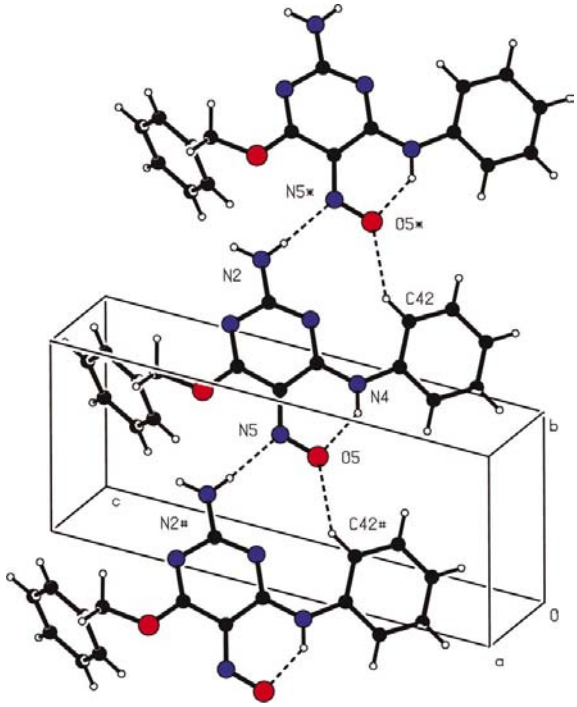

Figure 14
Part of the crystal structure of (5) showing the formation of a $[\bar{1}10]$ chain. The atoms marked with an asterisk (*) or a hash (#) are at the symmetry positions $(-1+x, 1+y, z)$ and $(1+x, -1+y, z)$, respectively.

3.2.6. 2-Amino-4-(*N*-benzylamino)-6-benzyloxy-5-nitrosopyrimidine (6). The structure of (6), which crystallizes in space group $P2_1/n$ with $Z' = 2$, has been discussed in previous papers (Quesada, Low *et al.*, 2002; Quesada, Marchal *et al.*, 2002): suffice it to note here that the supramolecular aggregation arises from the cooperative combination of N—H···N and N—H···π(arene) hydrogen bonds giving chains generated by 2_1 screw axes, as in (2).

3.2.7. 2-Amino-4-(*N*-butylamino)-6-(3-pyridyl)methoxy-5-nitrosopyrimidine (7). Compound (7) (Fig. 15) is closely related to (2), although differing from (2) in having a 6-(3-pyridyl)methoxy substituent in place of the 6-benzyloxy substituent typical of the rest of the series of compounds studied here. The supramolecular aggregation in (7), in contrast to that not only in (2) but to the rest of this series also, is dominated by the participation of the 2-amino group in two N—H···N hydrogen bonds. The 2-amino group in the molecule at (x, y, z) acts as a hydrogen-bond donor, *via* H2*A* and H2*B*, respectively, to nitroso N5 in the molecule at $(x, 1-y, \frac{1}{2}+z)$, and to pyridine N63 in the molecule at $(x, 2-y, \frac{1}{2}+z)$. Individually, these two hydrogen bonds produce $C(7)$ and $C(10)$ chains, generated, respectively, by the *c*-glide planes at $y = 0.5$ and $y = 1$: together they generate a (100) sheet in the form of a (4,4) net (Batten & Robson, 1998) built from a single type of $R_4^4(28)$ ring (Fig. 16). There is a single C—H···O hydrogen bond, which lies within the (100) sheet and thus simply reinforces this sheet: aromatic C62 at (x, y, z) acts as a donor to nitroso O5 at $(x, 1+y, z)$, so generating by translation a $C(9)$ chain parallel to [010].

The reference sheet lies in the domain $0.01 < x < 0.26$, and four such sheets pass through each unit cell: pairs of sheets related by inversion are linked into bilayers by aromatic $\pi\cdots\pi$ stacking interactions. The pyridine rings in the molecules at (x, y, z) and $(-x, 2-y, -z)$ are parallel with an interplanar spacing of 3.423 (2) Å; the centroid separation is 3.677 (2) Å, corresponding to a centroid offset of 1.343 (2) Å (Fig. 17). There are thus two bilayers passing through each unit cell, in

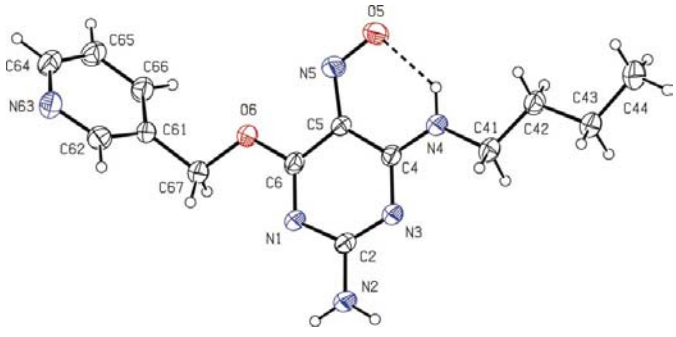

Figure 15
View of a molecule of (7) showing the atom-labelling scheme. Displacement ellipsoids are drawn at the 30% probability level.

the domains $-0.26 < x < 0.26$ and $0.24 < x < 0.76$, related to one another by the C-centring operation.

3.2.8. 2-Amino-6-benzyloxy-4-piperidino-5-nitrosopyrimidine monohydrate (8). The secondary amino substituent at position 4 precludes the formation of any intramolecular N—H···O hydrogen bond in (8). Unusually in this series, (8) crystallizes as a monohydrate (Fig. 18) and the water molecule acts as a double donor and as a single acceptor of hydrogen bonds, and is thus an integral component of the supramolecular structure. The pyrimidine molecules alone form chains and these chains are linked into sheets by the water molecules. Amino N2 in the molecule at (x, y, z) acts as a hydrogen-bond donor, *via* H2*A*, to nitroso N5 in the molecule at $(-1 + x, y, z)$, so generating by translation the now familiar

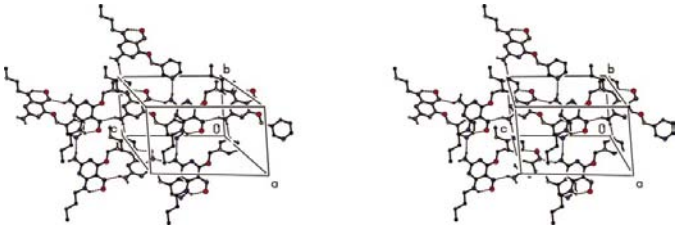

Figure 16
Stereoview of part of the crystal structure of (7) showing the formation of a (100) sheet of $R_4^4(28)$ rings. For the sake of clarity H atoms bonded to C are omitted.

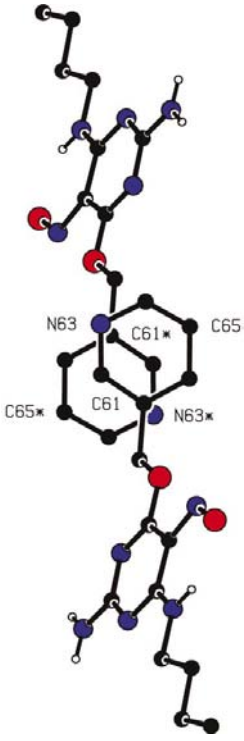

Figure 17
Part of the crystal structure of (7) showing the $\pi\cdots\pi$ stacking interaction between pyridine rings. For the sake of clarity H atoms bonded to C are omitted. The atoms marked with an asterisk (*) are at the symmetry position $(-x, 2 - y, -z)$.

C(7) chain, on this occasion running parallel to the [100] direction. Four of these chains pass through each unit cell and chains related by 2_1 screw axes are linked into sheets by the water molecules.

Within the asymmetric unit (Fig. 18), amino N2 acts as a hydrogen-bond donor, *via* H2*B*, to the water O1. Water O1 at (x, y, z) acts as a donor, *via* H1*A* to nitroso O5 in the pyrimidine at $(2 - x, \frac{1}{2} + y, \frac{1}{2} - z)$, so producing a $C_2^2(10)$ chain, generated by the 2_1 screw axis along $(1, y, \frac{1}{4})$: the same water molecule also acts as a donor, *via* H1*B*, to pyrimidine N3 at $(1 - x, \frac{1}{2} + y, \frac{1}{2} - z)$, so producing a $C_2^2(6)$ chain, generated by the 2_1 screw axis along $(\frac{1}{2}, y, \frac{1}{4})$. The combination of the [100] chain and the two [010] chains generates a (001) sheet in the form of a (3,6) net (Batten & Robson, 1998) built from $R_3^3(9)$ and $R_5^5(19)$ rings, alternating in checkerboard fashion (Fig. 19). The reference sheet lies in the domain $-0.06 < z < 0.56$ and a second sheet, related to the first by inversion, lies in the domain $0.44 < z < 1.06$: there are neither C—H···π(arene) interactions nor aromatic $\pi\cdots\pi$ stacking interactions in the structure of H and hence there are no direction-specific interactions between adjacent (001) sheets.

3.2.9. 2-Amino-6-benzyloxy-4-piperidino-pyrimidine (9). Compound (9) is a close analogue of (8), but having no nitroso substituent: the crystallization characteristics of (9) differ from those of (8) in that (9) does not crystallize as a hydrate and it has $Z' = 2$. Each molecule acts as a double donor and as a double acceptor in N—H···N hydrogen bonds. Within the asymmetric unit (Fig. 20), amino N12 and N22 act as hydrogen-bond donors, *via* H12*A* and H22*B*, to N21 and N13, respectively, so forming an $R_2^2(8)$ ring. In addition, N12 and N22 at (x, y, z) also act as donors, *via* H12*B* and H22*A*, to N23 at $(-1 + x, y, z)$ and to N11 at $(1 + x, y, z)$, respectively, so forming a second $R_2^2(8)$ ring. The overall supramolecular structure is thus a chain of edge-fused $R_2^2(8)$ rings generated by

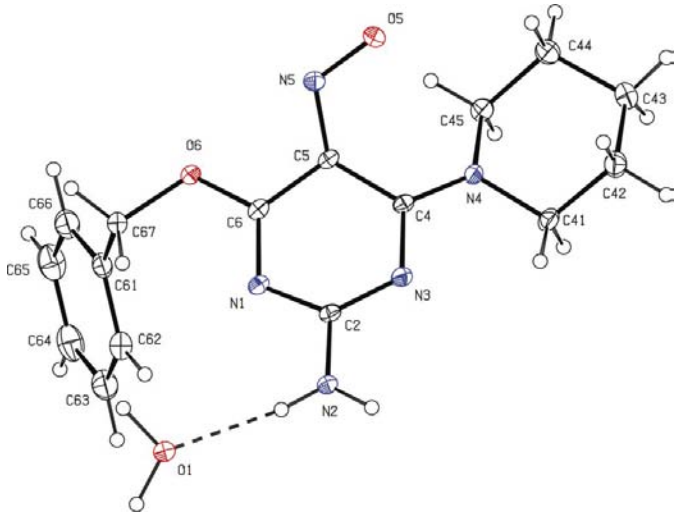

Figure 18
View of the molecular components of (8) showing the atom-labelling scheme. Displacement ellipsoids are drawn at the 30% probability level.

translation along [100] (Fig. 21). This structure may alternatively be regarded as a molecular ladder, having two distinct $C_2^2(6)$ chains acting as the uprights and the C12—N12 and C22—N22 bonds acting as the rungs of the ladder. The disposition of the piperidino and benzyloxy substituents on the edges of the chain of rings precludes any possibility of additional symmetry: likewise the dimensions of the hydrogen bonds (Table 4) show that in each type of $R_2^2(8)$ ring, one of the hydrogen bonds has H···N and N···N distances which are significantly longer than those of the other, although the two rings are quite similar to each other.

3.2.10. General comments on the supramolecular structures. Each of compounds (1)–(7) forms an intramolecular N—H···O hydrogen bond in which the nitroso O acts as the acceptor. In addition, the supramolecular structures of these compounds may contain either or both of two types of hard intermolecular hydrogen bond, those of N—H···N and N—H···O types, and these may be accompanied by any of three types of soft intermolecular hydrogen bond, those of C—H···O, C—H···π(arene) and N—H···π(arene) types, although C—H···N interactions are entirely absent from this series. Despite this absence, there are in a number of compounds [specifically (3)–(5)] N—H bonds for which no plausible hydrogen-bond acceptor can be identified.

In (1), where any steric effects generated by the N^4-substituent are expected to be minimal, there are both N—H···N and N—H···π(arene) hydrogen bonds, as well as C—H···O and C—H···π(arene) interactions, so that all of the N—H bonds have acceptors: including the intramolecular bond, the acceptors *A* in the N—H···*A* hydrogen bonds are O, N and arene, respectively.

The same set of acceptors are present in the N—H···*A* hydrogen bonds for (2), and in (6) (Quesada, Marchal *et al.*, 2002), where the N^4-substituent groups are somewhat larger, but C—H···*A* hydrogen bonds are wholly absent, while in (3) containing a long-chain N^4-substituent not only are C—H···*A* hydrogen bonds absent, but there are now no N—H···π(arene) hydrogen bonds, so that H2*B* has no acceptor. This is also the case in both of compounds (4) and (5), where the N^4 substituent is also more bulky than methyl or *n*-butyl, although the structures of these compounds contain C—H···π(arene) and C—H···O hydrogen bonds, respectively, although neither arene ring in (5) acts as an acceptor. In (7), on the other hand, where there is an additional acceptor N in the pyridyl substituent, this N acts as an acceptor for H2*B*; hence, in the isoelectronic and isosteric pair (2) and (7), the presence of the additional hard acceptor in (7) effectively replaces the N—H···π(arene) hydrogen bond in (2) by a stronger N—H···N hydrogen bond.

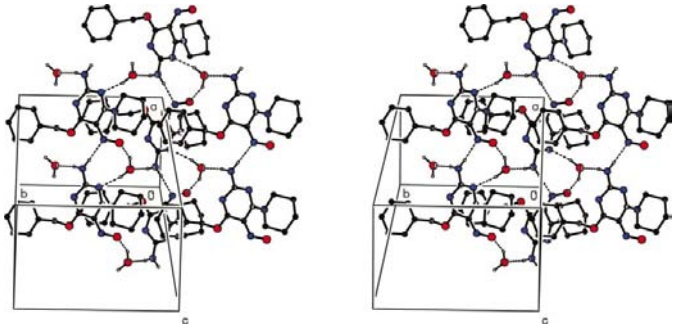

Figure 19
Stereoview of part of the crystal structure of (8) showing the formation of a (001) sheet of $R_3^3(9)$ and $R_5^5(19)$ rings. For the sake of clarity, H atoms bonded to C are omitted.

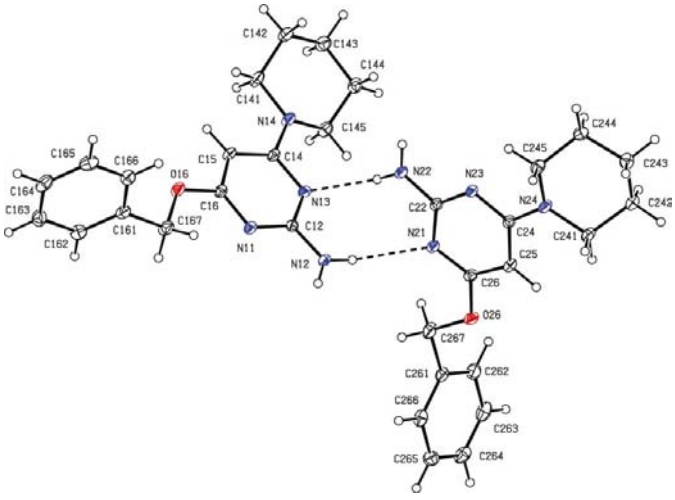

Figure 20
View of the two independent molecules of (9) showing the atom-labelling scheme and the hydrogen bonds within the asymmetric unit. Displacement ellipsoids are drawn at the 30% probability level.

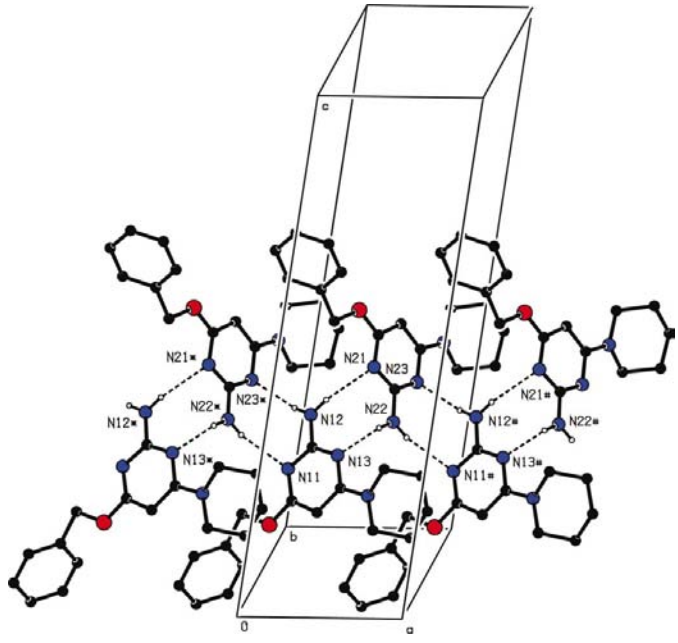

Figure 21
Part of the crystal structure of (9) showing the formation of a chain of edge-fused $R_2^2(8)$ rings along [100]. For the sake of clarity, H atoms bonded to C are omitted. The atoms marked with an asterisk (*) or hash (#) are at the symmetry positions $(-1+x, y, z)$ and $(1+x, y, z)$, respectively.

In (8) and (9) containing a piperidino substituent at N4, there can be no intramolecular N—H···O hydrogen bond. Compound (8) crystallizes as a monohydrate with $Z' = 1$, and the amino group at N2 forms both an N—H···O hydrogen bond, with water O as the acceptor, and an intermolecular N—H···N hydrogen bond with nitroso N as the acceptor: both of the water O—H bonds find acceptors in the form of the nitroso O and a pyrimidine ring N, respectively. In the absence of the nitroso substituent, (9) crystallizes with $Z' = 2$, but without any co-crystallized solvent molecules. In (9), all of the pyrimidine ring N atoms act as acceptors in intermolecular N—H···N hydrogen bonds. It may be noted that in (1)–(7), the pyrimidine ring N atoms, which are all potential hydrogen-bond acceptors, play no role whatsoever in the hydrogen bonding: in (1) and (2), as already noted, much weaker N—H···π(arene) hydrogen bonds are present, in preference to N—H···N interactions with pyrimidine N acceptors, while in each of (3)–(5) there is an N—H bond which finds no acceptor at all. The absence of such acceptor behaviour on the part of the pyrimidine ring N atoms in so many compounds of this series is particularly unexpected since such atoms are clearly competitive as hydrogen-bond acceptors with nitro O atoms in the supramolecular aggregation of 2-amino-4,6-dimethoxy-5-nitropyrimidine and 4-amino-2,6-dimethoxy-5-nitropyrimidine (Glidewell *et al.*, 2003).

4. Concluding comments

The differing manifestations, in (1)–(8) of a range of hard and soft hydrogen bonds, along with aromatic $\pi\cdots\pi$ stacking interactions in some cases, are such that no two compounds within this series of very closely related pyrimidines exhibit the same types of direction-specific intermolecular interactions. Much effort continues to be expended in attempts to compute, using a variety of *ab initio*, semi-empirical and heuristic methods, the structures of simple molecular compounds (Lommerse *et al.*, 2000; Motherwell, 2001; Motherwell *et al.*, 2002). However, weak forces of the types manifest here, dependent upon molecular polarizability and polarization, are not easy to model computationally, as the detailed charge distribution within molecules not only influences the expression of the weak intermolecular forces, but in turn may itself depend in a subtle way on the detailed molecular environment. The variations in the supramolecular aggregation behaviour within an extended series of related compounds, such as those described here, provides a keen test of computational methods for crystal-structure prediction, and the accurate prediction of behaviour across such a series would generate real confidence in the efficacy of the predictive method employed. On the other hand, the unexpected differences between the crystal structures within series such as that reported here and elsewhere (Farrell *et al.*, 2002; Glidewell *et al.*, 2002), together with the entire phenomenon of polymorphism, in particular the rather frequent observation of concomitant polymorphism (Bernstein *et al.*, 1999), raise at least the suspicion that for systems characterized by weak and/or long-range intermolecular forces the crystal structures may, in general, be intrinsically non-computable.

X-ray data were collected at the EPSRC X-ray Crystallographic Service, University of Southampton, UK, using a Nonius Kappa-CCD diffractometer. The authors thank the staff for all their help and advice. JNL thanks NCR Self Service, Dundee, for grants which have provided computing facilities for this work.

References

Batten, S. R. & Robson, R. (1998). *Angew. Chem. Int. Ed.* **37**, 1460–1494.
Bauer, S. H. & Andreassen, A. L. (1972). *J. Phys. Chem.* **76**, 3099–3108.
Bernstein, J., Davey, R. J. & Henck, J.-O. (1999). *Angew. Chem. Int. Ed.* **38**, 3440–3461.
Boeyens, J. C. A. (1978). *J. Cryst. Mol. Struct.* **8**, 317–320.
Cremer, D. (1984). *Acta Cryst.* B**40**, 498–500.
Cremer, D. & Pople, J. A. (1975). *J. Am. Chem. Soc.* **97**, 1354–1358.
Davis, M. I., Boggs, J. E., Coffey, D. & Hanson, H. P. (1965). *J. Phys. Chem.* **69**, 3727–3730.
Evans, D. G. & Boeyens, J. C. A. (1989). *Acta Cryst.* B**45**, 581–590.
Farrell, D. M. M., Glidewell, C., Low, J. N., Skakle, J. M. S. & Zakaria, C. M. (2002). *Acta Cryst.* B**58**, 289–299.
Ferguson, G. (1999). *PRPKAPPA*. University of Guelph, Canada.
Flack, H. D. (1983). *Acta Cryst.* A**39**, 876–881.
Flack, H. D. & Bernardinelli, G. (2000). *J. Appl. Cryst.* **33**, 1143–1148.
Gilli, P., Bertolasi, V., Ferretti, V. & Gilli, G. (1994). *J. Am. Chem. Soc.* **116**, 909–915.
Glidewell, C., Howie, R. A., Low, J. N., Skakle, J. M. S., Wardell, S. M. S. V. & Wardell, J. L. (2002). *Acta Cryst.* B**58**, 864–876.
Glidewell, C., Low, J. N., Melguizo, M. & Quesada, A. (2003). *Acta Cryst.* C**59**, o14–o18.
Gordy, W. (1947). *J. Chem. Phys.* **15**, 305–310.
Kotelevskii, S. I. & Prezhdo, O. V. (2001). *Tetrahedron*, **57**, 5715–5729.
Lommerse, J. P. M., Motherwell, W. D. S., Ammon, H. L., Dunitz, J. D., Gavezzotti, A., Hofmann, D. W. M., Leusen, F. J. J., Mooij, W. T. M., Price, S. L., Schweizer, B., Schmidt, M. U., van Eijck, B. P., Verwer, P. & Williams, D. E. (2000). *Acta Cryst.* B**56**, 697–714.
Marchal, A., Sánchez, A., Nogueras, M. & Melguizo, M. (1998). 18th European Colloquium on Heterocyclic Chemistry, Rouen, France. Abstract B-42.
Marchal, A., Sánchez, A., Nogueras, M. & Melguizo, M. (2000). 7th Ibn Sina International Conference on Pure and Applied Heterocyclic Chemistry, Alexandria, Egypt. Abstract P-214.
Motherwell, W. D. S. (2001). *Mol. Cryst. Liq. Cryst.* **356**, 559–567.
Motherwell, W. D. S., Ammon, H. L., Dunitz, J. D., Dryabchenko, A., Erk, P., Gavezzotti, A., Hofmann, D. W. M., Leusen, F. J. J., Lommerse, J. P. M., Mooij, W. T. M., Price, S. L., Scheraga, H., Schweizer, B., Schmidt, M. U., van Eijck, B. P., Verwer, P. & Williams, D. E. (2002). *Acta Cryst.* B**58**, 647–661.
Nonius (1997). *Kappa-CCD Server Software*. Windows 3.11 Version, Nonius BV, Delft, The Netherlands.
Otwinowski, Z. & Minor, W. (1997). *Methods Enzymol.* **276**, 307–326.
Quesada, A., Low, J. N., Melguizo, M., Nogueras, M. & Glidewell, C. (2002). *Acta Cryst.* C**58**, o355–o358.
Quesada, A., Marchal, A., Melguizo, M., Nogueras, M., Sánchez, A., Low, J. N., Cannon, D., Farrell, D. M. M. & Glidewell, C. (2002). *Acta Cryst.* B**58**, 300–315.
Quesada, A., Marchal, A., Sánchez, A., Nogueras, M. & Melguizo, M. (2000). XIXth Eur. Colloquium on Heterocyclic Chemistry, Aveiro, Portugal. Abstracts, p. 227.
Schlemper, E. O., Murmann, R. K. & Hussain, M. S. (1986). *Acta Cryst.* C**42**, 1739–1743.

Sheldrick, G. M. (1997*a*). *SHELXL*97. University of Göttingen, Germany.
Sheldrick, G. M. (1997*b*). *SHELXS*97. University of Göttingen, Germany.
Spek, A. L. (2002). *PLATON*. Version of June 2002. University of Utrecht, The Netherlands.
Talberg, H. J. (1977). *Acta Chem. Scand. A*, **31**, 485–491.
Wilson, A. J. C. (1976). *Acta Cryst.* A**32**, 994–996.